Analysis of MOX Critical Experiments with JENDL-3.3

Takako SHIRAKI, Hideki MATSUMOTO and Makoto NAKANO
Reactor Core Engineering Department, Mitsubishi Heavy Industries, Ltd.,
3-1, Minatomirai 3-chome, Nishi-ku Yokohama 220-8401
e-mail:shiraki@atom.hq.mhi.co.jp

This paper reports a study to confirm the applicability of the latest version of Japanese Evaluated Nuclear Data Library (JENDL3.3[1)]). For this purpose, the criticality calculations using MCNP4C[2)] code are performed to evaluate middle and high plutonium content MOX (M-MOX(8.6 w/o (Pu/MOX))) and H-MOX(12.6 w/o (Pu/MOX))) experiments (VIP, VIPO and VIPEX) using the JENDL3.3. Afterward, the same calculations with ENDF/B-6[3)] release 8 (ENDF/B-6.8) are performed to be compared with the results from JENDL3.3. Recently, ORNL have reevaluated U235 and U238 cross-sections in thermal and resonance energy[4)]. Those new evaluations are stored in ENDF/B-pre7. The effect of the U235 and U238 cross-sections on both JENDL3.3 and ENDF/B-6.8 are evaluated. The results clarify that JENDL3.3 is superior to ENDF/B-6.8 although both libraries underestimate the criticality. In addition, the ENDF/B-pre7 data for U235 and U238 solves the underestimation.

1. Introduction

Mitsubishi Heavy Industries, Ltd. joined R&D international programs on MOX experiments in collaboration with the Japanese PWR utilities with the objective to validate the design codes for MOX utilization. Some programs were carried out using VENUS critical facility at the SCK/CEN in Belgium from 1990 to 1998. The criticality experiments were performed for middle- and high-plutonium content MOX (M-MOX(8.6 w/o (Pu/MOX))) and H-MOX(12.6 w/o (Pu/MOX))).

JENDL has not been used in the design of PWR core design, except for decay heat evaluations by the ORIGEN-2 code. In 2002, JENDL3.3 was released, based on the update measurement data than ENDF/B-5 or B-6. It is necessary for us to confirm the applicability of JENDL3.3 from the viewpoint of future application of the JENDL3.3 or later version of JENDL in core design.

In this study, to confirm the applicability of JENDL3.3, we performed benchmarking-calculations using Monte Carlo code against the test data from the VENUS facility.

2. Criticality experiment programs

The experiment data used for the benchmark calculations were obtained from the VENUS critical assembly at SCK/CEN of Belgium. The VIP was carried out as a mock up simulation of MOX and UO2 PWR assemblies. The VIPO was performed to investigate the characteristics of the core with high void fraction. The VIPEX was carried out 6 years after the VIP to measure the effect of Am or other substance using the same core configuration as the VIP.

Table 1 shows the fuel specifications used by these programs. These are three kinds of MOX fuel and two kinds of UO2 fuel. The plutonium content of the low-plutonium content MOX (L-MOX) fuel is 4.8 w/o. The MOX fuel claddings are made of Zircaloy-4. The fuel active length is 100 cm. The contents of U235 enrichment of UO2 fuel are 3.3 w/o and 4.0 w/o, respectively. Both fuel active lengths are 50 cm. The claddings of 3.3 w/o UO2 fuel and 4.0 w/o UO2 fuel are made of Zircaloy-4 and stainless steel, respectively.

Table 1 Fuel specifications

		Fuel type				
		H-MOX	M-MOX	L-MOX	3.3 w/o	4.0 w/o
Fuel	Pu/MOX or U235/U (w/o	12.6	8.6	4.8	3.3	4
	Diamter (cm)	0.82			0.82	0.89
	Hight(MOX+UO2) (cm)	100+3.6			0+50	
	Density (g/cm^3)	10.11	10.13	10.17	10.25	10.21
Cladding	Material	Zr-4	Zr-4	Zr-4	Zr-4	Stainless steel
	Diamter (cm)	0.963			0.95	0.978
	Thickness (cm)	0.061			0.057	0.038

The VIP core consists of one central 17 x 17 MOX fuel-bundle and four peripheral 17 x 17 3.3 w/o UO2 fuel rod bundles. These bundles are surrounded by about three rod layers with 4.0 w/o UO2 fuel. The cell pitch is 1.26cm. Aluminum microtubes and microrods are inserted between MOX fuel rods and 3.3 w/o UO2 fuel rods at the corner of each square unit cell to simulate the density of high temperature water in PWR core. The VIP configuration is shown in **Fig. 1**. The VIPEX configuration is the same as that of the VIP.

The VIPO core consists of a 14 x 14 MOX fuel assembly, surrounded by 11 rod layers of 3.3 w/o UO2 fuel and 6 rod layers of 4.0 w/o UO2 fuel as shown in **Fig.2**. The cell pitch is 1.26cm. The two rods outer layers of the MOX fuel assembly consist of H-MOX fuel, while the 10 x 10 inner part consists either of H-MOX fuel or M-MOX fuel rods. The VIPO has used a void box to simulate the void fraction between the fuel rods. This box is made of Lexan whose density is 1.2 g/cm^3. The height of the voided region is 15 cm and this region encloses a 10 x 10 fuel rod in the center of the core.

In these experiments, critical water level, horizontal- and axial-power distributions, and other parameters were measured. These power distributions were obtained with γ-scanning method.

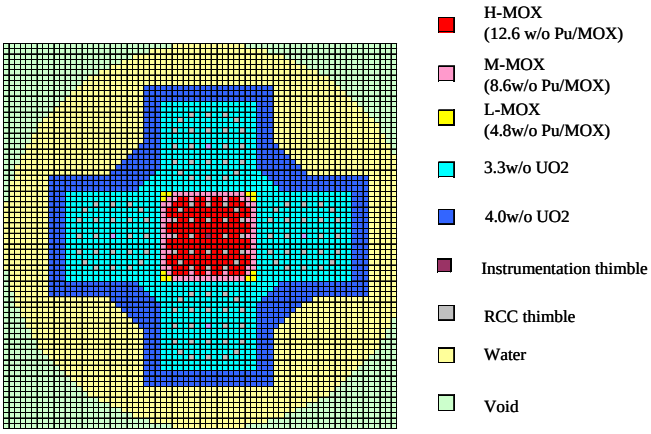

Fig.1 Cross-section view of VIP and VIPEX model

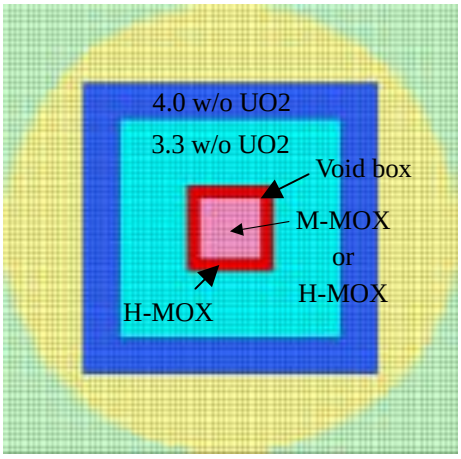

Fig.2 Cross-section view of VIPO model

3. Calculation conditions

The calculation code we used is the Monte Carlo N-Particle transport code, MCNP4c3. Our calculation models cover horizontal-cross section from the core center to the water region outside of core and axial-cross section from the lower support to the upper support.

The VIP and the VIPEX calculation models are shown in **Fig. 3**. In this model, each fuel cell includes fuel, cladding, Al-microrod, Al-microtube and water. The upper and intermediate grids are modeled considering the heterogeneity. Since the core configurations are of one-eighth symmetry, correspondingly we employed one-eighth symmetry for the calculation. Pu241 decays to Am241 by β-decay with a half life of 14.4 years. Therefore VIPEX Pu241 composition decreases to 77 % and Am241 composition increases to 158 % as compared with those of the VIP.

The VIPO calculation model is shown in **Fig. 4**. The four calculations are performed on the VIPO program. These are the M-MOX fuel in the center region with a void box, the H-MOX fuel in the center region with a void box, the M-MOX fuel in the center region without a void box and the H-MOX fuel in the center region without a void box. These water levels are 146.71cm, 146.02cm, 145.47cm, 144.72cm, respectively. Since each fuel rod of VIPO is the same as that of VIP, the axial modeling such as upper, intermediate and upper grid is the same as the VIP.

In these analyses, the five kinds of cross-sections are applied as shown in **Table 2**.

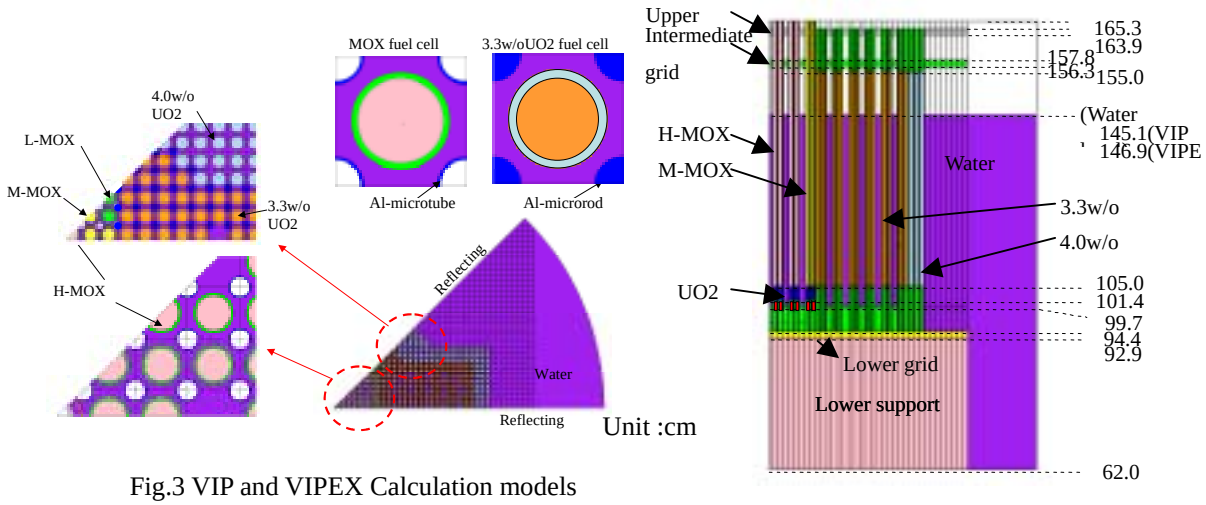

Fig.3 VIP and VIPEX Calculation models

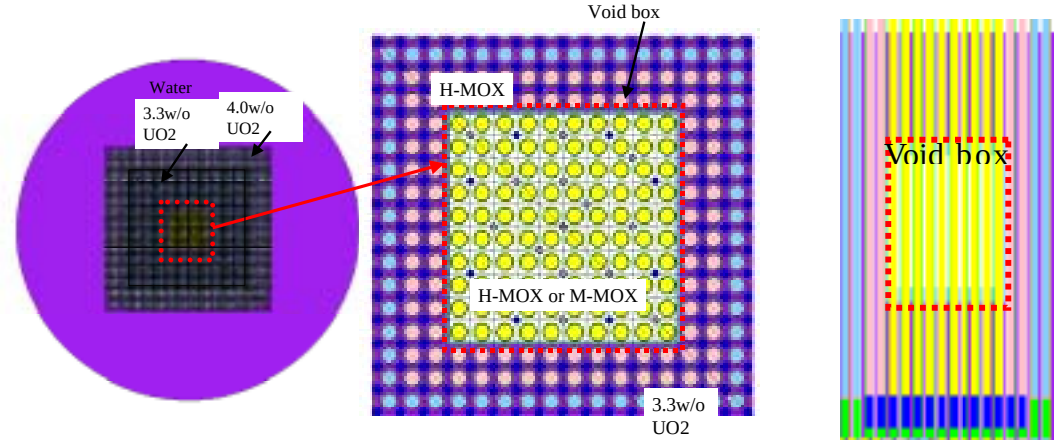

Horizontal cross section Axial cross section

Fig.4 VIPO calculation model

The multiplication factors are calculated with the MCNP function, “KCODE”. The horizontal and axial power distributions are calculated with “F4 tally” which can evaluate reaction rates, etc. in each cell.

4. Calculation results

4.1 Neutron multiplication factors

Table 3 shows the calculated results for the neutron multiplication factors (keff). Each calculation standard deviation is less than 0.04%. The mean keff of VIP, VIPO and VIPEX obtained from JENDL3.3 is 0.9943, and the keff obtained from ENDF/B-6.8 is 0.9911. From the viewpoint of criticality evaluation for MOX, we find JENDL3.3 is superior to ENDF/B-6.8. Although both libraries slightly underestimate the keff's, the standard deviations within the 6 calculation

Table2 Cross section sets

Nuclide	JENDL3.3	JENDL3.3+ ENDF/B-pre7(U235,U238)	JENDL3.3+ ENDF/B-pre7(H1,O16, U235,U238)	ENDF/B-6.8	ENDF/B-pre7
H1	JENDL3.3	JENDL3.3	ENDF/B-6.r8	ENDF/B-6.r8	ENDF/B-6.r8
O16	JENDL3.3	JENDL3.3	ENDF/B-6.r8	ENDF/B-6.r8	ENDF/B-6.r8
U234	JENDL3.3	JENDL3.3	JENDL3.3	ENDF/B-6.2	ENDF/B-6.2
U235	JENDL3.3	ENDF/B-pre7	ENDF/B-pre7	ENDF/B-6.r5	ENDF/B-pre7
U236	JENDL3.3	JENDL3.3	JENDL3.3	ENDF/B-6.1	ENDF/B-6.1
U238	JENDL3.3	ENDF/B-pre7	ENDF/B-pre7	ENDF/B-6.r5	ENDF/B-pre7
Pu238	JENDL3.3	JENDL3.3	JENDL3.3	ENDF/B-6.2	ENDF/B-6.2
Pu239	JENDL3.3	JENDL3.3	JENDL3.3	ENDF/B-6.r2	ENDF/B-6.r2
Pu240	JENDL3.3	JENDL3.3	JENDL3.3	ENDF/B-6.r2	ENDF/B-6.r2
Pu241	JENDL3.3	JENDL3.3	JENDL3.3	ENDF/B-6.r3	ENDF/B-6.r3
Pu242	JENDL3.3	JENDL3.3	JENDL3.3	ENDF/B-6.2	ENDF/B-6.2
Am241	JENDL3.3	JENDL3.3	JENDL3.3	ENDF/B-6.r3	ENDF/B-6.r3

cases are as small as 0.0008 and 0.0009 for JENDL3.3 and ENDF/B-6.8, respectively. It shows that good accuracy is maintained throughout the core configurations including those with large void and H-MOX fuel and M-MOX fuel.

By using ENDF/B-pre7 U235 and U238 data instead of original ones for these nuclides, the keff's with JENDL3.3 and ENDF/B-6.8 libraries increase by about 160pcm and 520pcm, respectively. The different effects of the new ENDF/B-pre7 cross-sections made JENDL3.3 and ENDF/B-6.8 consistent with each other, both giving the keff's of about 0.996. By using the ENDF/B-6.8 data for H1 and O16 instead of JENDL3.3 ones, the keff's decrease by about 130pcm.

Fig. 5 shows the ratio of neutron flux with each cross-section sets to that with JENDL3.3 in the fuel of the VIP. It can be seen ENDF/B-6.8 gives the most hard spectrum. The flux with ENDF/B-6.8 is larger by 1% over 9.1keV and less by 0.6% under 9.1keV comparing with that with JENDL3.3. On the other hand, the other cases are in good agreement. The differences are less than 0.2% for all energy ranges.

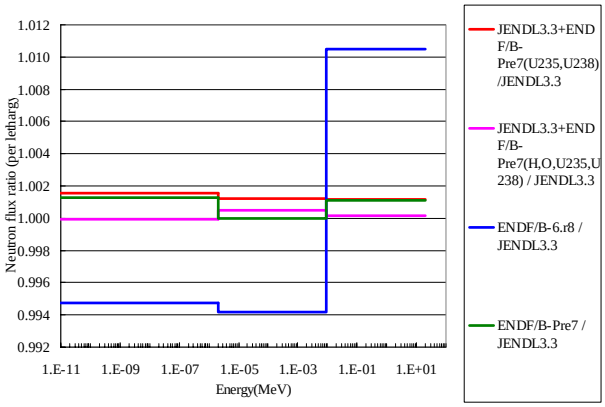

Fig.5 Ratio of neutron flux with each cross-section set to that with JENDL3.3 in the fuel (VIP)

Table 3 Multiplication factors in VIP, VIPEX and VIPO analyses with each library

	VIP	VIPEX	VIPO				
	keff	keff	10×10 M-MOX with void box	10×10 H-MOX with void box	10×10 M-MOX without void box	10×10 H-MOX without void box	Mean
Cross section			keff	keff	keff	keff	keff
①JENDL3.3	0.99471	0.99535	0.99444	0.99448	0.99321	0.99368	0.99431 ± 0.0008
②JENDL3.3+ ENDF/B-pre7(U235,U238)	0.99707	0.99808	0.99765	0.99738	0.99631	0.99665	0.99719 ± 0.0007
③JENDL3.3+ ENDF/B-pre7(H1,O16,U235,U238)	0.99571	0.99646	0.99589	0.99699	0.99515	0.99503	0.99587 ± 0.0008
④ENDF/B-6.8	0.99114	0.99253	0.99114	0.99174	0.99003	0.99016	0.99112 ± 0.0009
⑤ENDF/B-pre7	0.99552	0.99749	0.99592	0.99689	0.99556	0.99633	0.99629 ± 0.0008
Difference (pcm)							
②-①	237	274	322	291	312	298	289
③-①	100	111	146	252	195	136	157
⑤-④	441	498	481	518	557	621	519

Table 4 Mean C/E's of horizontal power distribution with each library in VIP and VIPO

Cross section	VIP				VIPO					
	MOX assembly		UO2 assembly		MOX assembly				UO2 assembly	
					In void box		Out void box			
	C/E ave.	1σ	C/E ave.	1σ	C/E ave.	1σ	C/E ave.	1σ	C/E ave.	1σ
①JENDL3.3	1.015	0.009	0.984	0.011	0.999	0.025	1.019	0.026	0.978	0.011
②JENDL3.3+ ENDF/B-Pre7(U235,U238)	1.016	0.016	0.983	0.017	1.005	0.031	1.019	0.069	0.982	0.031
③JENDL3.3+ ENDF/B-Pre7(H1,O16,U235,U238)	1.015	0.020	0.983	0.018	1.003	0.047	1.014	0.039	0.981	0.036
④ENDF/B-6.8	1.014	0.015	0.986	0.016	0.986	0.036	1.018	0.040	0.980	0.038
⑤ENDF/B-pre7	1.016	0.016	0.982	0.015	0.993	0.035	1.034	0.048	0.970	0.027

4.2 Power distribution

Table 4 shows the C/E mean values for each region with each library in the VIP and the VIPO. In the VIP, the γ intensity of 50 fuel rods in MOX region and 59 fuel rods in UO2 region were measured for horizontal power distributions. The uncertainty of measured value in MOX fuel and UO2 fuel are less than 1.8 % and 1.4 %, respectively.

In the VIPO, the γ intensity of 13 fuel rods inside the void box, 15 fuel rods outside the void box in the MOX fuel region and 28 fuel rods in UO2 region were measured for horizontal power distributions. The uncertainty of measured value is less than 1.5 %. The measured values (E) and the calculated values (C) with each library are compared in each fuel rod. **Fig.6** shows the comparison of horizontal power distribution between measurements and calculations with JENDL3.3 as example. This model is the M-MOX fuel in the center region with a void box

The calculation standard deviations are less than 0.8%. The differences with each library are small. Although the calculated values agree with the measured values within the measured and calculated errors, the C/E's in the MOX region tend to be larger than these in the UO2 region.

The axial power distributions in the VIPO H-MOX rods with the void box and 3.3 w/o UO2 fuel rods are shown in **Fig.7**. The uncertainty of measured value is less than 2%. The calculation standard deviations are less than 2%. The differences between measured and calculated values are not so large in the void box. The

calculated values are lower than the measured values by about 5 % at the maximum in the void box. These distributions agree within 3% in the UO2 fuel.

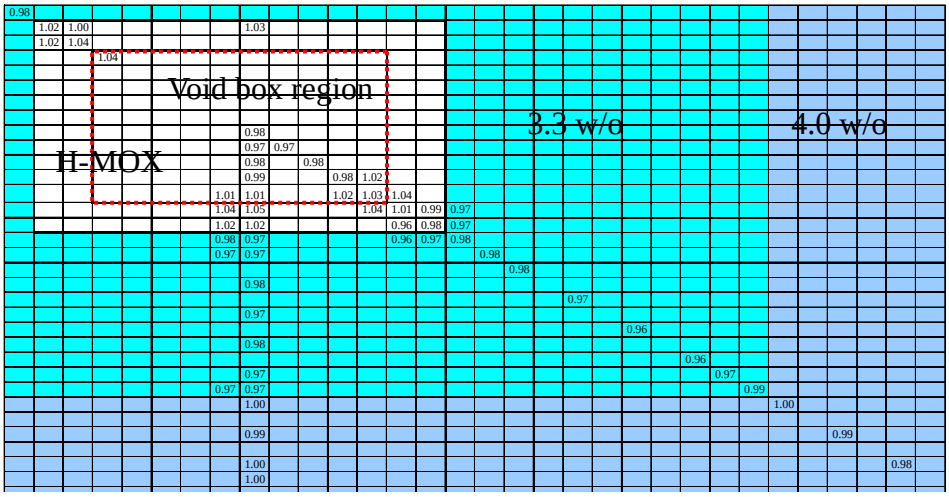

Fig.6 Comparison of horizontal power distributions with JENDL3.3 in VIPO (C/E)

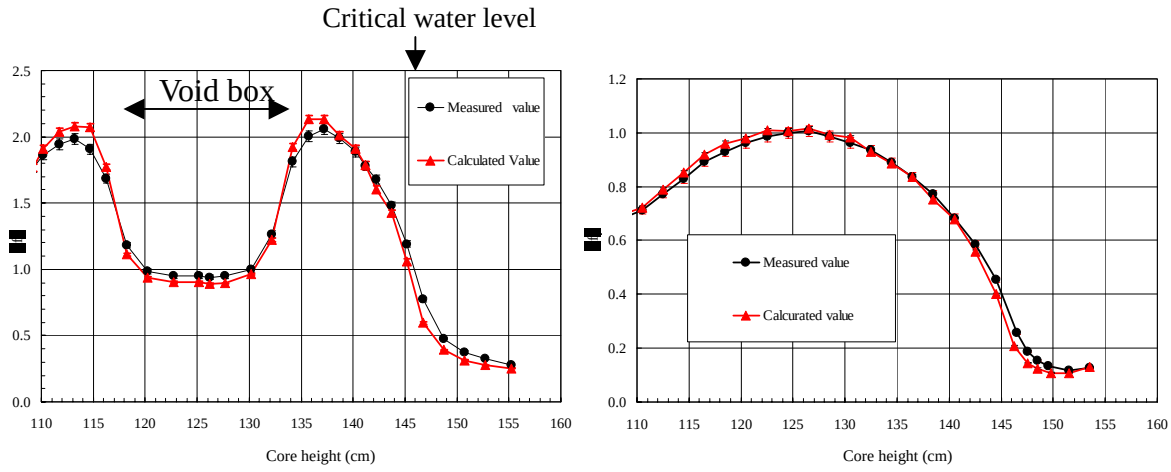

H-MOX fuel inside of void box

UO2 fuel

Fig.7 Axial power distributions in VIPO

5. Discussion

By using ENDF/B-pre7 U-235 and U-238 data instead of the original ones, the keff's increase by about 290pcm and 520pcm for JENDL3.3 and ENDF/B-6.8, respectively. The different effect of ENDF/B-pre7 data on keff for JENDL3.3 and ENDF/B6.8 is discussed here.

Fig.8 shows the differences of capture and fission reaction rates of all fuel rods in the VIP with the ENDF/B-pre7 data for U235 and U238 from the original cross-section sets. The U238 capture rates are decreased when the ENDF/B-pre7 data for both libraries use. The difference in the rate for JENDL3.3 is twice larger than for ENDF/B-6.8. The U235 capture rates are increased. The difference in the rate on JENDL3.3 is twice smaller than on ENDF/B-6.8. On the other hand, the U235 fission rates are increased. The difference in the rate on JENDL3.3 is three times smaller than on ENDF/B-6.8. The capture and fission rates of other isotopes change through neutron spectrum change by using the ENDF/B-pre7 data for U235 and U238. **Fig.9** shows that those differences result in the total production, absorption and leakage rates for both libraries. The difference of total absorption including leakage by using the ENDF/B-pre7 data for U235 and U238 becomes small. It shows that the differences cancel out among isotopes. On the other hand, the difference of U235 fission reaction rate remains in total production rates. This is the cause of the difference in reactivity change due to the U235 and U238 ENDF/B-pre7 data. This increases the calculated keff of ENDF/B-6 more than JENDL3.3. As the result, keff obtained by JENDL3.3 with the ENDF/B-pre7 data for U235 and U238 agree well with ENDF/B-pre7.

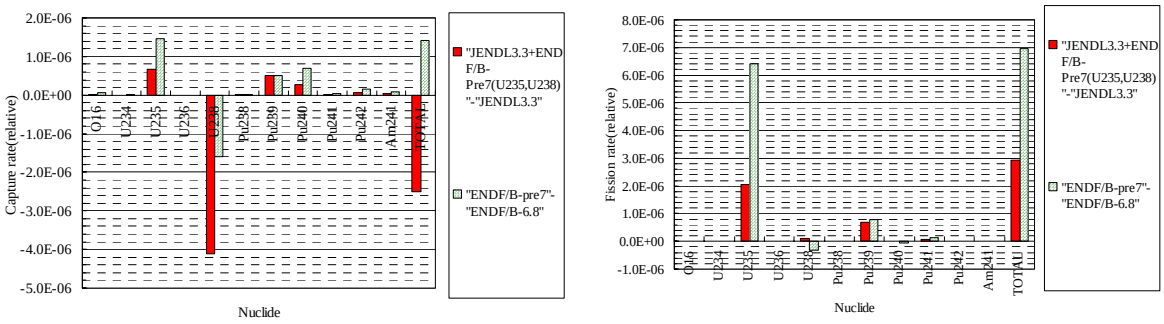

Fig.8 Reaction rate effect of ENDF/B-pre7 for U235 and U238 data

6. Summary

This paper reports a study to confirm the applicability of the JENDL3.3. For this purpose, the criticality calculations using MCNP4C code are performed to evaluate M-MOX and H-MOX experiments (VIP, VIPO and VIPEX) using the JENDL3.3. Afterward, the same calculations with ENDF/B-6.8 are performed. Recently, ORNL have reevaluated U235 and U238 cross-sections in thermal and resonance energy. The effect of the U235 and U238 cross-sections on both JENDL3.3 and ENDF/B-6.8 are evaluated.

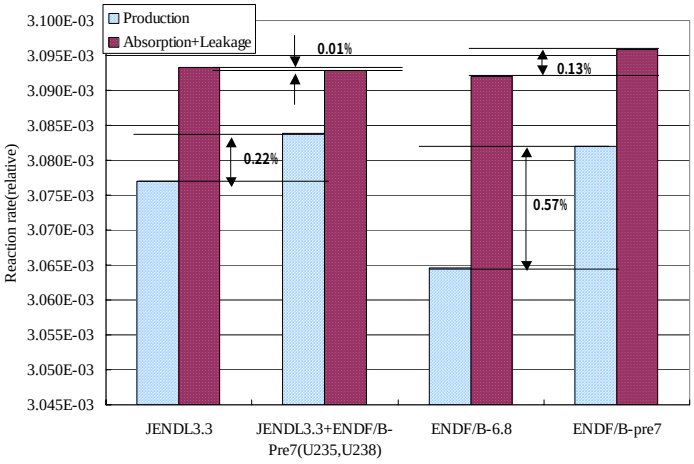

Fig.9 Detail of reaction rates

As for power distribution, the calculated values agree with the measured values within the measured and calculated errors for all calculated cases. However the C/E's of power distribution in the MOX region tend to be larger than those in the UO2 region. The tendency may improve when re-evaluation of plutonium cross-section will be performed in the future.

Although the JENDL3.3 and ENDF/B-6.8 underestimate the criticality, JENDL3.3 is superior to ENDF/B-6.8. The ENDF/B-pre7 data for U235 and U238 solves the underestimation.

We expect that U235 and U238 should be re-evaluated in the future JENDL-4 as performed for ENDF/B-pre7.

7. References

[1] K.Shibata, et al., "Japanese Evaluated Nuclear Data Library Version 3 Revision-3: JENDL-3.3," J. Nucl. Sci. Technol., 39, 1125(2002).

[2] Los Alamos National Laboratory Los Alamos, New Mexico "MCNP4C: Monte Carlo N-Particle Transport Code System," CCC-700(April 2000).

[3] P. F. Rose, Ed., "ENDF-201, ENDF/B-VI Summary Documentation," BNL-NCS-17541,4th Edition, Brookhaven National Laboratory (October 1991).

[4] Los Alamos National Laboratory T-2 Nuclear Information Service, http://t2.lanl.gov/data/data/preVII-neutron/U/.